
COHERENT BEAM COMBINATION OF TEN FIBER ARRAYS VIA STOCHASTIC PARALLEL GRADIENT DESCENT ALGORITHM

© 2015 Z. Huang^{*}; X. Tang^{**}; D. Zhang^{*}; X. Wang^{**}; Q. Hu^{*}; J. Li^{*}; C. Liu^{*}

^{*}Institute of Fluid Physics, China Academy of Engineering Physics, Mianyang, China

^{**}Institute of Applied Physics and Computational Mathematics, Beijing, China

E-mail: zhimenghuang@126.com

Coherent beam combination of ten fiber arrays using a stochastic parallel gradient descent (SPGD) algorithm is demonstrated. A high speed phase controller has been designed and manufactured based on SPGD algorithm and a field programmable gate array (FPGA). The signal processing speed of the FPGA circuit is 50 MHz and its iteration rate is more than 200 kHz. Experimental investigation on coherent beam combination of 10 fiber laser beams is successfully demonstrated, with imposing an additional phase disturbances to mimic the phase noises in the high power fiber amplifiers. The combining efficiency is about 96.4% and 92.6% without/with additional phase distortion, corresponding to the RMS phase error of $\lambda/35$ and $\lambda/23$.

Key words: fiber arrays, coherent beam combination, stochastic parallel gradient descent algorithm.

OCIS codes: 140.0140; 140.3298, 140.3290.

1. Introduction

The high power coherent beam combination (CBC) system with active phase-locking of master oscillator power amplifier (MOPA) array has a great potential to achieve high brightness and maintain a good beam quality [1–5]. There are mainly three kinds of active phasing methods, i.e., a heterodyne phase detecting [6–8], a multi-dithering technique [9, 10], and a stochastic parallel gradient descent (SPGD) algorithm [11, 12]. CBC with the heterodyne detection phase control technique requires a reference beam and a photo-detector array with the same element numbers as the beamlets in the whole MOPA system, and the system becomes increasingly complex and sophisticated when scaled to a large number of arrays. The multi-dithering technique needs one photo-detector, and the phase control can be implemented at a high speed, but every element in the array requires an individual phase modulation frequency and corresponded phase control module; accordingly

the modulation frequency accumulates to an extremely high value and becomes difficult to practically implement with an increase in the beamlet numbers. A CBC system based on the SPGD optimization algorithm needs only one photo-detector and no phase detecting while generating phase control, which is simple, compact, and has the potential to be scaled to a large-scale array with high output power and good beam quality, embedded with the capability of fast beam steering.

In this paper, a coherent beam combination of ten fiber arrays via SPGD algorithm is demonstrated experimentally. The signal processing speed of the FPGA control circuit is 50 MHz, and its iteration rate is more than 200 kHz. In the experiment, an active phase locking of 10 fiber laser beams is successfully obtained, with imposing an additional phase disturbances to mimic phase noises in high power fiber amplifiers. The combining efficiency with the modulated phase noise is achieved above 92.6%, and the accuracy of the phase control is improved to $\lambda/23$ RMS.

2. Theory

2.1. Principle of stochastic parallel gradient descent algorithm

SPGD control algorithm is one of image sharpening techniques in Adaptive Optics (AO). It develops from a Simultaneous Perturbation Stochastic Approximation (SPSA) control algorithm. This technique has been successfully realized in astronomical AO observation systems and Free Space Optics communication. In MOPA coherent combining system based on SPGD control algorithm, the independence of wave-front sensor makes the configuration immensely simplified. The algorithm corrects the piston errors automatically by a characteristic-value optimization. Comparing with the Hill-Climbing algorithm, SPGD algorithm develops from being serial to parallel. This development brings a higher rate of convergence when the number of MOPA channels increases. The manual setting gain provides the rate and precision of convergence being under control [13].

In our 10-channel MOPA system, the generic SPGD algorithm is customized by the following functions:

(1) Using the encircle energy in the diffraction limit of combined wave-front as the performance metric $J^{(k)}$.

(2) Generating statistically independent random voltage perturbations $\delta u_i^{(k)}$, where $|\delta u_i^{(k)}|$ are small constants.

(3) Adding these voltage perturbations on phase modulators positively and evaluate the performance metric:

$$J_+^{(k)} = J(u_1^{(k)} + \delta u_1^{(k)}, u_2^{(k)} + \delta u_2^{(k)}, \dots, u_{10}^{(k)} + \delta u_{10}^{(k)}). \quad (1)$$

(4) Adding these voltage perturbations on phase modulators negatively and evaluate the performance metric:

$$J_-^{(k)} = J(u_1^{(k)} - \delta u_1^{(k)}, u_2^{(k)} - \delta u_2^{(k)}, \dots, u_{10}^{(k)} - \delta u_{10}^{(k)}). \quad (2)$$

(5) Calculating the difference between these two metrics:

$$\delta J^{(k)} = J_+^{(k)} - J_-^{(k)}. \quad (3)$$

(6) Updating the feedback control voltage:

$$u_i^{(k+1)} = u_i^{(k)} + \gamma \delta u_i^{(k)} \delta J^{(k)}. \quad (4)$$

Here k represents the iteration number, i is the channel number, and γ represents the algorithm gain. The parameter γ can be either adaptive or constant. For our simulation, it is suitable for us-

ing a constant gain to demonstrate the capability of correction. When γ is positive, $J^{(k)}$ is a maximum for the constructive interference; otherwise, it is a minimum for the destructive interference.

2.2 Far-field diffraction model

A far-field of the coherent combining is the Fraunhofer diffraction:

$$E(x, y) = (c/f) \exp \left[ik \left(f + \frac{x^2 + y^2}{2f} \right) \right] \times \times \iint_{\Sigma} E(x_1, y_1) \exp \left[-\frac{ik}{f} (xx_1 + yy_1) \right] dx_1 dy_1. \quad (5)$$

Here λ represents the wavelength, Σ represents the aperture area, f represents the focus distance, $c = 1/i\lambda$; $k = 2\pi/\lambda$, and $E(x_1, y_1)$ represents the complex amplitude of the aperture area, $E(x, y)$ represents the complex amplitude of the far-field image plane. The expression (5) gives a relation of the complex amplitude distributing between two planes: if the complex amplitude of the aperture area is known, it's possible to calculate the far-field complex amplitude by 2D Fast Fourier Transform (FFT) algorithm, which means the physical process of diffraction could be simulated in PC [13].

3. Experimental setup

To demonstrate a feasibility of the square wave dithering technique, an experiment of a coherent beam combination of ten beams is performed utilizing a dual-level phase dithering method. The system architecture is shown in fig. 1.

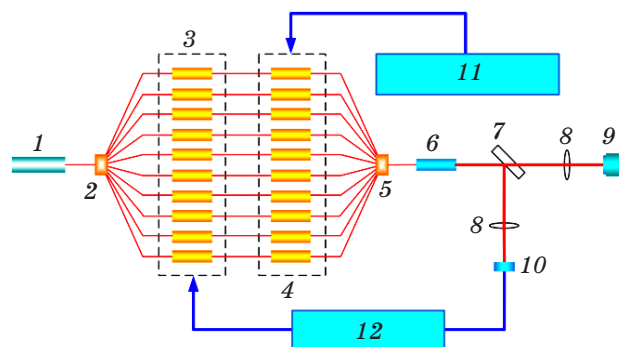


Fig. 1. (Color online) Schematic of system architecture for coherent combining of ten beams with additional phase distortion. 1 – master oscillator; 2 – splitter; 3 – phase controller; 4 – phase modulator; 5 – combiner; 6 – collimator; 7 – sampler; 8 – lens; 9 – CCD; 10 – photodetector; 11 – distortion generator; 12 – signal processing.

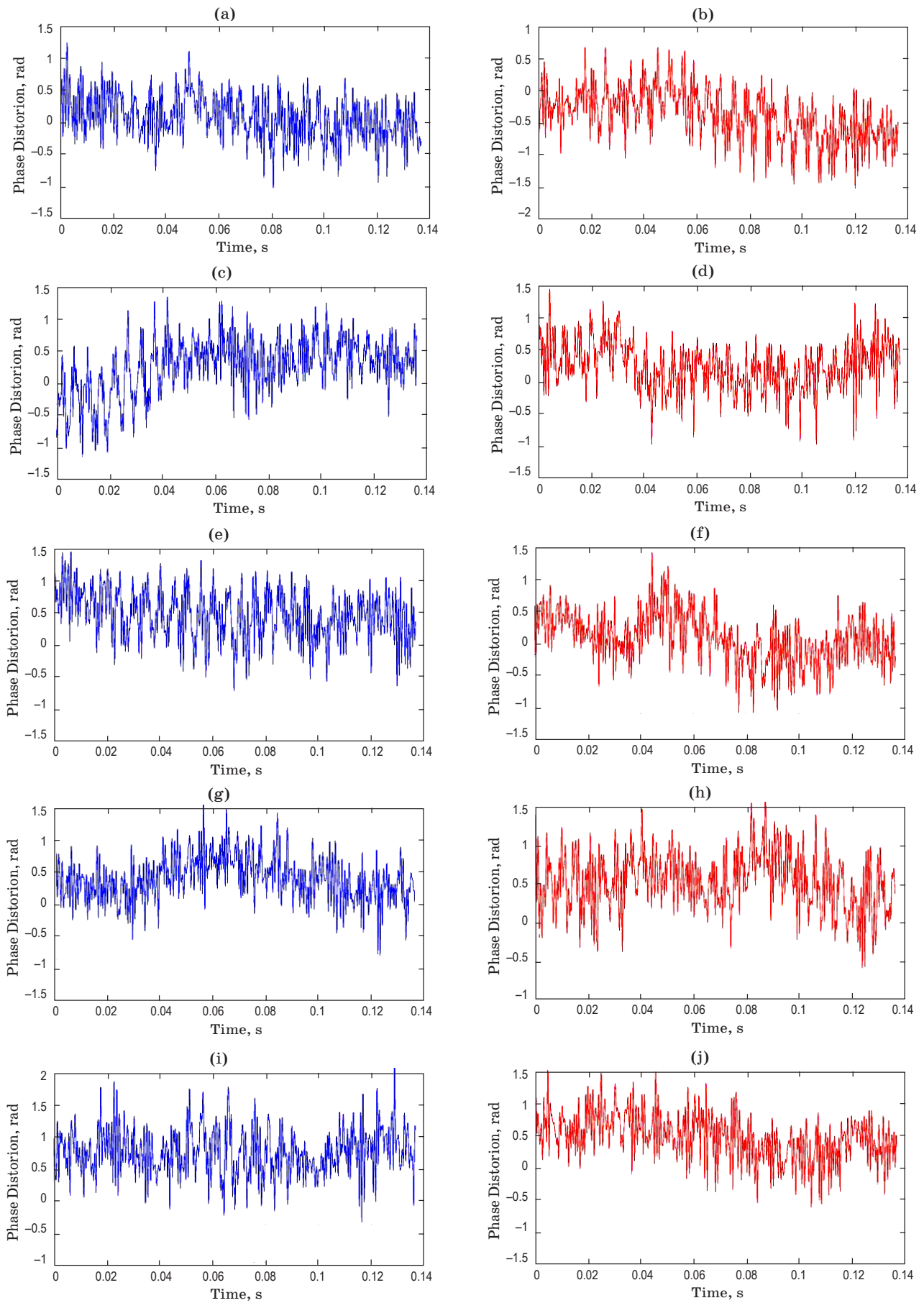


Fig. 2. Additional phase distortions in one cycle period. (a–j) phase evaluation of ten different beams.

The seed laser is a single frequency polarization maintaining (PM) fiber laser at the wavelength of 1064 nm with the line-width of 1 kHz. The output power of the seed laser through the optical isolator is about 250 mW. The laser beam is split into ten beams and coupled to ten LiNbO3 phase controllers. The output PM fibers of the phase controller are connected to similar polarization maintaining phase modulators. The phase modulators are used to generate phase distortions that mimic the phase noises of the fiber amplifiers. Although to emulate the phase noise in this way has some difference from being accurate, it is good enough to demonstrate the technical feasibility of phase-locking in our experiments. The ten fiber outputs are combined via an integrated PM beam combiner. The combiner is used to replace other optics architecture used in high power system such as diffractive optical element [14]. After combination, the light passes through a fiber-coupled beam collimator with 14 mm diameter of output beam and then is split by a 50:50 beam splitter. The transmitted branch goes through a lens with a focal length of 1 m, then into a CCD camera. The reflected branch goes through a lens which also has a focal length of 1 m, then into a photo-detector placed at focus plane. The photo-detector is an InGaAs amplifier detector with 700–1800 nm response wavelength, 800 μm aperture size, and 17 MHz bandwidth when the gain is at 0 dB. The output electric signal of photo-detector is send to a signal processing circuit based on FPGA, which provides a 200 kHz dual-level phase dithering as the time-division phase modulation signal [15].

In general, the phase noises can be expanded by a cosine function basis as

$$\phi(t) = \sum_{n=1}^{\infty} A_n \cos(2n\pi\Delta vt). \quad (6)$$

We assume the additional phase noises of different channels have the similar spectral density of phase noise but different time variation behavior. It is realized by taking the same absolute value but random signs of the coefficient A_n to capture the stochastic feature of the phase noise. In the experiment, we use an arbitrary wave generator to generate the wideband phase noises. In practice, the phase distortions are 10-bits digitalized in the range of $[-\pi, \pi]$, and cyclic with fix period length T , that is $\phi(t + T) = \phi(t)$, and t belongs to $[0, T)$, where $T = 0.1365$ s.

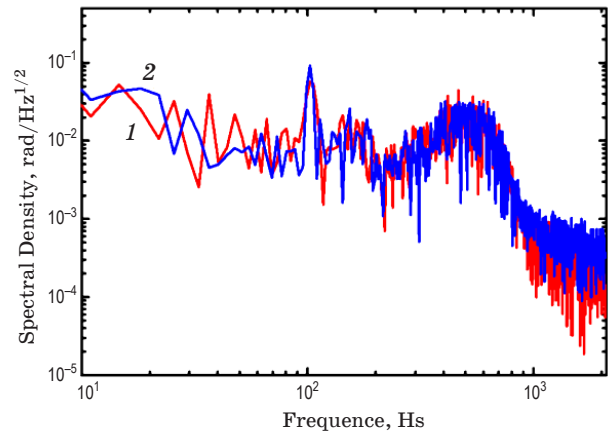


Fig. 3. Additional phase distortions spectral density. 1 – channel 1; 2 – channel 2

The phase distortions (ten samples in one cycle period T) are shown in fig. 2. The corresponding spectral density curves of the additional phase distortion in fig. 2(a) and fig. 2(b) are shown in fig. 3, which are similar to the experimental results [16]. It should be noticed that the spectral density functions represent a part of phase noises contributed by additional modulation only, but the practical phase noise also includes those induced by environment such as a mechanical quivering [15].

4. Results and discussion

The time series signals of the photo-detector are also presented to compare the system performance in an open loop and a closed loop, as shown in fig. 4. In the open loop, the combined beam intensity fluctuates randomly. Additionally imposed phase distortions increase the frequency of intensity fluctuation.

The Strehl SR ratio SR evaluating the coherent efficiency can be estimated by the following formula [17]:

$$\text{SR} = \exp(-\sigma^2) + \left[1 - \exp(-\sigma^2)\right] / N \quad (7)$$

σ is the root-mean-square (RMS) of phase error. It can be further divided into

$$\sigma^2 = \sigma_M^2 + \sigma_{\text{corr}}^2 + \sigma_{\text{res}}^2, \quad (8)$$

Here σ_M is induced by the phase modulation, σ_{corr} is the RMS of the phase correction error, and σ_{res} is caused by a non-real time phase correction, which is a positive correlation with the time delay of phase control, and can be obtained from the structure function of the phase change [16].

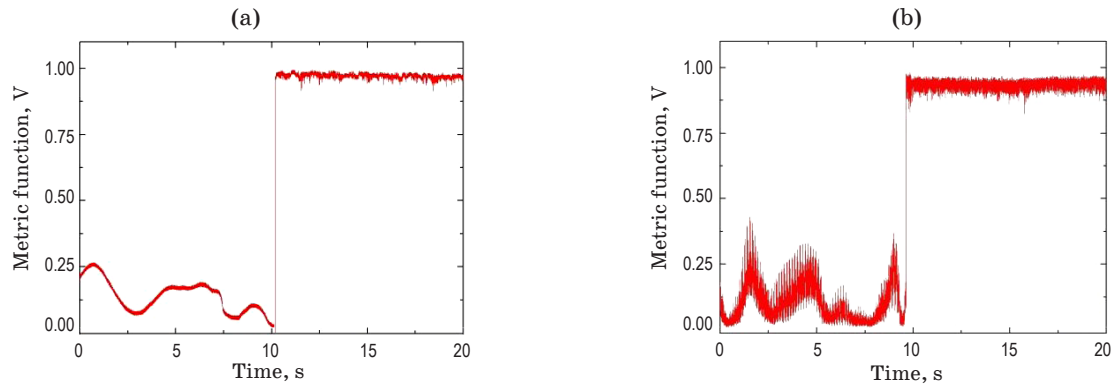


Fig. 4. (Color online) Time series signals of the photo-detector in the open loop and the closed loop using SPGD: (a) without the additional phase distortion, (b) with the additional phase distortion.

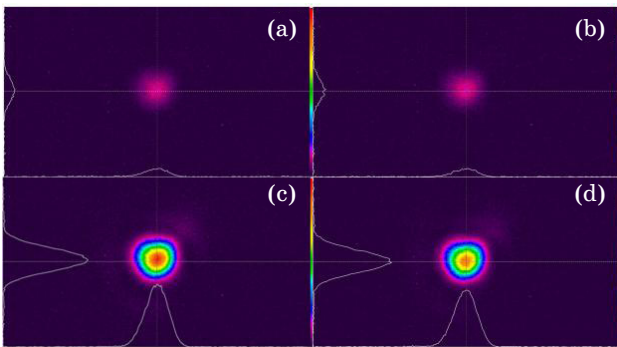


Fig. 5. Far-field intensity pattern of the combined laser beam (a) without additional phase distortion in open loop, (b) with additional phase distortion in open loop, (c) without additional phase distortion in close loop, (d) with additional phase distortion in close loop.

We carry out the SPGD method on the same system. In the closed loop, the intensity of the combined beam is locked steadily. The combining efficiency evaluated by the Strehl ratio is about 96.4% and 92.6% with/without the additional phase distortion, corresponding to the phase error of $\lambda/35$ RMS and $\lambda/23$ RMS. It indicates that effective coherent combination can be achieved for high-power performance.

Figure 5 shows typical far-field patterns without and with the additional phase distortions. In the open loop, the phases of channels are randomly varying due to an environment impact and phase distortion modulations. In closed loop,

* * * * *

the phase control algorithm is implemented. The intensity is boosted and steady at 32 Hz sample rate. The results demonstrate that effective coherent combinations are achieved.

5. Conclusion

In summary, the coherent beam combination of ten fiber arrays via SPGD algorithm is demonstrated. The signal processing speed of the FPGA control circuit is 50 MHz, and its iteration rate is more than 200 kHz. In the experiment, the active phase locking of 10 fiber laser beams is successfully obtained, with imposing an additional phase disturbances to mimic phase noises in high power fiber amplifiers. The combining efficiency with the modulated phase noise is achieved above 92.6%, and the accuracy of phase control is improved to $\lambda/23$ RMS. Along with the increase of the frequency of phase modulation signal, and the A/D and D/A converter speed, we believe the SPGD technique has a potential to be scaled to a large-scale array with high output power and good beam quality.

Acknowledgments

This work was supported by Key Laboratory of Science and Technology on High Energy Laser, CAEP, under Contract No. LJG2012-06 and the Development Foundation of IFP under No. SFZ20130302.

ЛИТЕРАТУРА

1. *Wagner T.J.* Fiber laser beam combining and power scaling progress // *Proc. SPIE*. 2012. V. 8505. P. 823718.
2. *Huang Z.M., Zhang D.Y., Luo Y.Q., Li J.F., Liu C.L.* A new configuration for phase control in laser coherent combination utilizing liquid crystal optical modulator // *Appl Phys B*. 2010. V. 101(3). P. 559–563.
3. *Huang Z.M., Liu C.L., Li J.F., Zhang D.Y., Wang Y.Q., Luo Y.Q., Hu Q.Q.* Numerical analysis of coherent combination for fiber lasers and application to beam steering // *Laser Physics*. 2012. V. 22 (8). P. 1347–1352.
4. *Huang Z., Tang X., Zhang D., Wang X., Li J., Liu C., Gao Q.* Phase locking of slab laser amplifiers via square wave dithering algorithm // *Appl. Opt.* 2014. V. 53(10). P. 2163–2169.
5. *Huang Z.M., Liu C.L., Li J.F., Zhang D.Y.* A high-speed high-efficiency phase controller for coherent beam combining based on SPGD algorithm // *Quantum Electronics*. 2014. V. 44 (4). P. 301–305.
6. *Augst S.J., Fan T.Y., Sanchez A.* Coherent beam combining and phase noise measurements of ytterbium fiber amplifiers // *Opt. Lett.* 2004. V. 29 (5). P. 474–476.
7. *Zhimeng H., Yongquan L., Dayong Z., Haitao L.* Active phase control in laser coherent combination based on liquid crystal optical modulator // *Chinese J. Lasers*. 2010. V. 37 (7). P. 1713–1716.
8. *Goodno G.D., Komine H., McNaught S.J., Weiss S.B., Redmond S., Long W., Simpson R., Cheung E.C., Howland D., Epp P., Weber M., McClellan M., Sollee J., Injeyan H.* Coherent combination of high-power, zigzag slab lasers // *Opt. Lett.* 2006. V. 31 (9). P. 1247–1249.
9. *Shay T.M., Benham V., Baker J.T., Ward B., Sanchez A.D., Culpepper M.A., Pilkington D., Spring J., Nelson D.J., Lu C.A.* First experimental demonstration of self-synchronous phase locking of an optical array // *Opt. Express* 2006. V. 14 (25). P. 12015–12021.
10. *Pulford B.N.* LOCSET phase locking: operation, diagnostics, and applications // Ph. D. dissertation. Univ. of New Mexico, 2011.
11. *Liu L., Vorontsov M.A.* Phase-locking of tiled fiber array using SPGD feedback controller // *Proc. SPIE*. 2005. V. 5895. P. 58950.
12. *Yu C.X., Augst S.J., Redmond S.M., Goldizen K.C., Murphy D.V., Sanchez A., Fan T.Y.* Coherent combining of a 4 kW, eight-element fiber amplifier array // *Opt. Lett.* 2011. V. 36 (14). P. 2686–2688.
13. *Zheng Y., Shen F.* Simulation and analysis of Stochastic Parallel Gradient Descent control algorithm for coherent combining // *Proc. SPIE*. 2009. V. 7156. P. 71563C.
14. *Redmond S.M., Ripin D.J., Yu C.X., Augst S.J., Fan T.Y., Thielen P.A., Rothenberg J.E., Goodno G.D.* Diffractive coherent combining of a 2.5 kW fiber laser array into a 1.9 kW Gaussian beam // *Opt. Lett.* 2012. V. 37 (14). P. 2832–2834.
15. *Tang X., Huang Z., Zhang D., Wang X., Li J., Liu C.* An active phase locking of multiple fiber channels via square wave dithering algorithm // *Opt. Commun.* 2014. V. 321. P. 198–204.
16. *Augst S.J., Ranka J.K., Fan T.Y., Sanchez A.* Beam combining of ytterbium fiber amplifiers (Invited) // *J. Opt. Soc. Am. B*. 2007. V. 24 (8). P. 1707–1715.
17. *Goodno G.D., Shih C.C., Rothenberg J.E.* Perturbation analysis of coherent combining efficiency with mismatched lasers // *Opt. Express*. 2010. V. 18 (24). P. 25403–25414.